

Direct observation of three-neutron emission from $^7\text{He}^*$ and the search for the trineutron

S. W. Huang^{1,2,3} C. Lenain⁴ Z. H. Yang^{1,2,*} F. M. Marqués⁴ J. Gibelin⁴ J. G. Li^{5,6,7} A. Matta⁴ N. A. Orr⁴ N. L. Achouri⁴ D. S. Ahn^{2,8,9} A. Anne⁴ T. Aumann^{10,11} H. Baba² D. Beaumel¹² M. Böhmer¹³ K. Boretzky^{11,2} M. Caamaño¹⁴ N. Chen^{5,6} S. Chen¹⁵ N. Chiga² M. L. Cortés² D. Cortina¹⁴ P. Doornenbal² C. A. Douma¹⁶ F. Dufter¹³ J. Feng¹ B. Fernández-Domínguez¹⁴ Z. Elekes^{17,18} U. Forsberg^{19,20} T. Fujino²¹ N. Fukuda² I. Gašparić^{22,2} Z. Ge² R. Gernhäuser¹³ J. M. Gheller²³ A. Gillibert²³ Z. Halász¹⁷ T. Harada^{2,24} M. N. Harakeh^{11,16} A. Hirayama^{25,2} N. Inabe² T. Isobe² J. Kahlbow^{10,2} N. Kalantar-Nayestanaki¹⁶ D. Kim⁸ S. Kim⁸ S. Kiyotake²⁶ T. Kobayashi²⁷ D. Koerper¹¹ Y. Kondo²⁵ P. Koseoglou^{10,11} Y. Kubota² I. Kuti¹⁷ C. Lehr^{10,2} P. J. Li^{28,15} Y. Liu¹ Y. Maeda²⁶ S. Masuoka²⁹ M. Matsumoto^{25,2} J. Mayer³⁰ N. Michel^{5,6} H. Miki²⁵ M. Miwa^{2,31} B. Monteagudo⁴ I. Murray² T. Nakamura¹⁰ A. Obertelli¹⁰ H. Otsu² V. Panin² S. Park⁸ M. Parlog⁴ S. Paschalis^{10,19} P. M. Potlog¹⁰ S. Reichert¹³ A. Revel^{33,4} D. Rossi^{10,11} A. T. Saito²⁵ M. Sasano² H. Sato² H. Scheit¹⁰ F. Schindler¹⁰ T. Shimada²⁵ Y. Shimizu² S. Shimoura²⁹ H. Simon¹¹ I. Stefan³⁴ S. Storck¹⁰ L. Stuhl^{29,8} H. Suzuki² D. Symochko¹⁰ H. Takeda² S. Takeuchi²⁵ J. Tanaka¹⁰ Y. Togano^{2,21} T. Tomai^{25,2} H. T. Törnqvist^{10,11} E. Tronchin⁴ J. Tscheuschner¹⁰ V. Wagner¹⁰ K. Wimmer²⁹ M. R. Xie^{5,6} H. Yamada²⁵ B. Yang¹ L. Yang²⁹ M. Yasuda^{25,2} Y. L. Ye¹ K. Yoneda² L. Zanetti^{10,2} J. Zenihiro^{2,35} and T. Uesaka²

¹School of Physics and State Key Laboratory of Nuclear Physics and Technology, Peking University, Beijing 100871, China

²RIKEN Nishina Center, Hirosawa 2-1, Wako, Saitama 351-0198, Japan

³Institute for Rare Isotope Science, Institute for Basic Science, Daejeon 34000, Republic of Korea

⁴Université de Caen Normandie, CNRS/IN2P3, ENSICAEN, LPC Caen, UMR6534, 14050 Caen Cedex, France

⁵Institute of Modern Physics, Chinese Academy of Sciences, Lanzhou 730000, China

⁶School of Nuclear Science and Technology, University of Chinese Academy of Sciences, Beijing 100049, China

⁷Southern Center for Nuclear-Science Theory (SCNT), Institute of Modern Physics, Chinese Academy of Sciences, Huizhou 516000, China

⁸CENS, Institute for Basic Science, Daejeon 34126, Republic of Korea

⁹Facility for Rare Isotope Beams, Michigan State University, East Lansing, MI 48824, USA

¹⁰Institut für Kernphysik, Technische Universität Darmstadt, D-64289 Darmstadt, Germany

¹¹GSI Helmholtzzentrum für Schwerionenforschung, 64291 Darmstadt, Germany

¹²Université Paris-Saclay, CNRS/IN2P3, IJCLab, 91405 Orsay, France

¹³Technical University of Munich, TUM School of Natural Sciences, 85747 Garching, Germany

¹⁴Departamento de Física de Partículas and IGFAE, Universidade de Santiago de Compostela, E-15782 Santiago de Compostela, Spain

¹⁵Department of Physics, The University of Hong Kong, Hong Kong, China

¹⁶ESRIG, University of Groningen, Zernikelaan 25, 9747 AA Groningen, The Netherlands

¹⁷Institute for Nuclear Research (HUN-REN ATOMKI), Debrecen, Hungary

¹⁸Institute of Physics, Faculty of Science and Technology, University of Debrecen, Egyetem tér 1, H-4032 Debrecen, Hungary

¹⁹School of Physics, Engineering and Technology, University of York, York YO10 5DD, United Kingdom

²⁰Department of Physics, Lund University, 22100 Lund, Sweden

²¹Department of Physics, Rikkyo University, 3-34-1, Nishi-Ikebukuro, Toshima, Tokyo 171-8501, Japan

²²Ruđer Bošković Institute (RBI), Zagreb, Croatia

²³Département de Physique Nucléaire, IRFU, CEA, Université Paris-Saclay, 91191 Gif-sur-Yvette, France

²⁴Department of Physics, Toho University, Funabashi, Chiba 274-8510, Japan

²⁵Department of Physics, Institute of Science Tokyo, 2-12-1 O-Okayama, Meguro, Tokyo 152-8551, Japan

²⁶Faculty of Engineering, University of Miyazaki, Miyazaki 889-2192, Japan

²⁷Department of Physics, Tohoku University, Aramaki Aza-Aoba 6-3, Aoba, Sendai, Miyagi 980-8578, Japan

²⁸Key Laboratory of Nuclear Physics and Ion-Beam Application (MOE), Institute of Modern Physics, Fudan University, Shanghai 200433, China

²⁹Center for Nuclear Study, University of Tokyo, 2-1 Hirosawa, Wako, Saitama 351-0198, Japan

³⁰Institut für Kernphysik, Universität zu Köln, Köln, Germany

³¹Department of Physics, Saitama University, Shimo-Okubo 255, Sakura-ku, Saitama-shi 338-8570, Japan

³²Institute of Space Science - INFLPR Subsidiary, Magurele, Romania

³³Grand Accélérateur National d'Ions Lourds (GANIL), CEA/DRF-CNRS/IN2P3, Bvd Henri Becquerel, 14076 Caen, France

³⁴Institut de Physique Nucléaire Orsay, IN2P3-CNRS, 91406 Orsay Cedex, France

³⁵Department of Physics, Kyoto University, Kitashirakawa, Sakyo, Kyoto 606-8502, Japan

*Contact author: zaihong.yang@pku.edu.cn

 (Received 11 August 2025; revised 15 December 2025; accepted 10 February 2026; published 1 April 2026)

Three-neutron emission from ${}^7\text{He}$ has been directly measured for the first time, following neutron knockout from a ${}^8\text{He}$ beam at 156 MeV/nucleon. A resonancelike structure at 2.08(4) MeV above the ${}^4\text{He} + 3n$ threshold [$E_x = 2.68(4)$ MeV] with a width of 3.9(2) MeV was observed and deduced to arise predominately from the predicted $J^\pi = 3/2^-$ level. The three-neutron invariant-mass spectrum was reconstructed and found to peak at around 1 MeV and could, through complete simulations incorporating neutron-neutron correlations, be very well described by the sequential decay of ${}^7\text{He}^*$ via the 2_1^+ excited state of ${}^6\text{He}$. No evidence was found for any significant three-neutron correlations beyond those expected from well-established two-body interactions, including a trineutron resonance.

DOI: [10.1103/sr8h-2n6v](https://doi.org/10.1103/sr8h-2n6v)

Introduction. Light nuclei with extreme neutron-to-proton asymmetry provide an ideal testing ground for our understanding of nuclei, including, in particular, the details of the two- and few-body forces used in models [1]. In this context, the search for the most extreme systems, such as multineutron clusters or resonances, has been the object in recent years, beginning with the measurement of Refs. [2,3], of significant experimental and theoretical efforts [4,5], and culminated with the recent observation of a near-threshold resonancelike structure in the $4n$ system [6,7]. It is, however, not yet clear whether this structure corresponds to a four-body resonance [8–12] or is the result of initial-state correlations in the projectile [13] and/or the reaction mechanism [14]. For the $3n$ system, the existence of a trineutron resonance has been predicted by *ab initio* calculations [10,12,15], but no evidence for any such relatively narrow structure has been found in high-statistics missing-mass experiments [16,17]. An important complementary means to search for multineutron systems is the direct detection of multiple neutron emission from well-defined states. Besides being independent of the projectile/initial state and the reaction, such direct detection has the potential to enable the investigation of multineutron correlations.

Significant progress has been made in investigating experimentally $2n$ and $2p$ emissions [18–30]. On the proton-rich side, several $3p$ emitters have been identified and studied [31–35] and two $4p$ emitters have been found [36,37]. In contrast, multineutron emission remains largely unexplored, owing primarily to the limited capabilities for detecting more than two neutrons. Recent advances in large-scale neutron arrays have enabled the direct detection of $3n$ and $4n$ emission from ${}^{27,28}\text{O}$ [38], both decaying sequentially through ${}^{26}\text{O}$ [39].

Neutron-rich helium isotopes, composed of an α core plus several valence neutrons, provide an ideal laboratory for exploring multineutron correlations. The ground state (g.s.) of ${}^6\text{He}$ exhibits pronounced dineutron clustering [42,43], and a strongly correlated four-neutron subsystem has been suggested to be present in the g.s. of ${}^8\text{He}$ in a recent ${}^8\text{He}(p, p\alpha)$ experiment [7]. Positioned between them, ${}^7\text{He}$ is thus a promising candidate for probing $3n$ correlations. While its g.s. is well established as a low-lying ${}^6\text{He} + n$ resonance with spin parity $J^\pi = 3/2^-$ [44–47], the excited states and their decay properties remain the subject of considerable debate [45–69]. Among them, a $3/2^-$ level above the $3n$ -emission threshold is of particular interest, since its J^π matches that favored in predictions for a possible trineutron resonance [10,12,15,70–

73], making trineutron emission a possible decay mode. A sequence of excited states ($1/2^-$, $5/2^-$, $3/2^-$) has been consistently predicted by a wide range of models, from the phenomenological shell model [50] to more sophisticated models including those incorporating the continuum [58–65]. Experimentally, however, evidence for these levels remains incomplete and sometimes contradictory. A narrow $1/2^-$ resonance at $E_x \sim 0.6$ MeV has been reported in high-energy breakup and (p, d) reactions on ${}^8\text{He}$ [56,57], but not observed in many other experiments [45–55]. Broader structures at $E_x \approx 2\text{--}3$ MeV have been suggested from neutron removal and isobaric-analog studies, with tentative $1/2^-$ or $5/2^-$ assignments [47–53]. Notably, none of these experiments detected all three neutrons, leaving the decay mechanism and possible signatures of $3n$ correlations unresolved.

In this Letter, we report on the first direct measurement of $3n$ emission from ${}^7\text{He}$ excited states populated using the ${}^8\text{He}(p, pn)$ reaction. High statistics and excellent invariant-mass resolution were achieved, by combining an intense ${}^8\text{He}$ beam, a thick liquid hydrogen target incorporating reaction vertex reconstruction, and a state-of-the-art neutron array. A resonancelike structure decaying exclusively into ${}^4\text{He} + 3n$ was observed and was identified as arising predominately from the $3/2^-$ level based on the momentum distribution of the knocked-out neutron and structure model predictions. The reconstructed $3n$ invariant-mass spectrum, as well as that for ${}^4\text{He} + 2n$, demonstrated that the $3n$ emission proceeds sequentially via ${}^6\text{He}^*(2_1^+)$. No evidence was found for any significant three-neutron correlations, including a trineutron resonance.

Experiment. The experiment was performed at the RI Beam Factory operated by the RIKEN Nishina Center for Accelerator-Based Science and CNS, the University of Tokyo. The ${}^8\text{He}$ secondary beam (156 MeV/nucleon, $\sim 10^5$ pps) was produced by fragmentation of an intense 220 MeV/nucleon ${}^{18}\text{O}$ beam on a Be target and purified using the BigRIPS fragment separator [74,75]. A schematic view and description of the setup can be found in Fig. 1. The secondary beam particles were tracked onto the 15 cm thick liquid hydrogen target of MINOS [76] using two drift chambers. The recoil protons from the (p, pn) reaction were tracked using a cylindrical time projection chamber surrounding the target, covering approximately $20^\circ\text{--}60^\circ$. Combined with the trajectory of the incident ${}^8\text{He}$ ions, this allowed for the reconstruction of the reaction vertex [77].

The charged fragments ${}^4,6\text{He}$ were momentum analyzed using the SAMURAI spectrometer [78,79]. The momenta

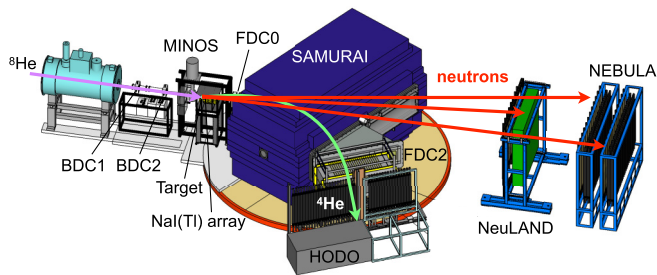


FIG. 1. Schematic view of the experimental setup. The incident ^8He beam was tracked by two drift chambers (BDC1, BDC2) onto the liquid hydrogen target system (MINOS). Recoil protons from the (p, pn) reaction were tracked using a cylindrical time projection chamber surrounding the target, and their energies were measured by an array of 36 NaI(Tl) crystals. The charged fragments ^4He (^6He) were momentum analyzed using the SAMURAI spectrometer and two drift chambers (FDC0, FDC2), and detected in a plastic scintillator array (HODO). The forward-going beam-velocity neutrons were detected by the multielene NeuLAND (single-wall) and NEBULA (two separated walls) plastic scintillator arrays, located approximately 11 and 14 m downstream of the target, respectively.

of forward-going neutrons were determined from their time-of-flight ($\sigma \approx 160$ ps) and hit positions measured by the NeuLAND [80] and NEBULA [81] plastic scintillator arrays. The combination of these two arrays (with a total thickness of 88 cm) improved significantly the multineutron detection efficiency, enabling the direct detection of three beam-velocity neutrons. Crosstalks—neutrons scattered within and detected more than once in the neutron arrays—were eliminated in the offline analysis using a rejection algorithm specifically developed for the present three-wall configuration [82,83].

The relative energies of the $^6\text{He} + n$, $^4\text{He} + 2n$, and $^4\text{He} + 3n$ decay channels were reconstructed from the momenta of the He fragments and the coincident decay neutrons using the invariant-mass method. The $1n$, $2n$, and $3n$ efficiencies varied smoothly with the relative energy (Fig. S1 in the Supplemental Material [84]), reaching some 40%, 14%, and 3%, respectively, at 1 MeV. The relative-energy spectra were fit using Breit-Wigner (BW) line shapes with energy-dependent widths for the resonances and a nonresonant contribution (arising from the nonresonant continuum and, for the $^4\text{He} + 2n$ channel, uncorrelated neutrons from the decay of ^7He to $^6\text{He}^*$) estimated using a simulation of the noninteracting $^4\text{He} + xn$ system [87]. All line shapes were input into a GEANT4 simulation of the complete setup, which incorporated the geometrical acceptances, efficiencies, and resolutions of the individual detectors, as well as the characteristics of the ^8He beam, target, and reaction effects. The simulated data were then analyzed in the same manner as the experimental data, including the crosstalk rejection. As such, the residual crosstalk contamination was included in the simulated spectra and was estimated to be $\sim 2\%$ for the $2n$ channel and $\sim 7\%$ for the $3n$ channel. The uncertainties reported below include both statistical and systematic components, with the latter evaluated by varying the fit range, parameters of the crosstalk rejection algorithm, and potential fragment-neutron momentum misalignments.

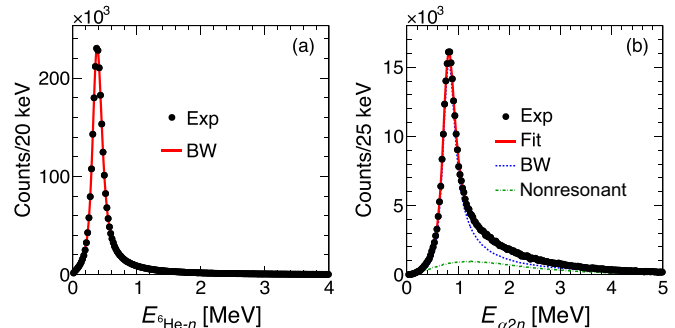


FIG. 2. Relative-energy spectra for (a) $^6\text{He} + n$ and (b) $^4\text{He} + 2n$ events. The red line shows the best fit (see text). The vertical error bars are statistical only.

One- and two-neutron channels. The $^6\text{He} + n$ relative-energy spectrum [Fig. 2(a)] exhibits a single narrow structure near threshold, corresponding to the well-known ^7He g.s. [44]. The resolution (FWHM), determined from simulations, varies as $\sim 0.16E_{^6\text{He}-n}^{0.57}$ MeV, and is 110 keV at $E_{^6\text{He}-n} = 0.5$ MeV. The spectrum is well described by a single $\ell = 1$ BW resonance with an energy of $E_r = 379(2)$ keV and a width of $\Gamma_r = 137(10)$ keV, in agreement with previous measurements of proton-induced neutron knockout from ^8He , albeit with a narrower width [45,46]. The high statistics and broad acceptance of this measurement have allowed us to rule out the population of any higher-lying resonances in this decay channel with a bin-by-bin significance well below 1σ (details in Ref. [84]).

The $\alpha + 2n$ spectrum [Fig. 2(b)] exhibits a narrow peak at ~ 0.8 MeV above threshold, corresponding to the well-known 2_1^+ state of ^6He [44]. The resolution varies as $\sim 0.17E_{\alpha 2n}^{0.56}$ MeV and is 150 keV at $E_{\alpha 2n} = 0.8$ MeV. The spectrum was fit up to 3 MeV using a combination of a BW resonance¹ and the nonresonant component described above. The red solid line shows the best fit, with $E_r = 823(6)$ keV and $\Gamma_r = 228(29)$ keV, in agreement with the known energy but with a broader width.

Three-neutron channel. The $^4\text{He} + 3n$ relative-energy spectrum (Fig. 3) exhibits a broad structure peaking at ~ 1.5 MeV. The resolution varies as $\sim 0.19E_{\alpha 3n}^{0.6}$ MeV. The spectrum was fit up to 5 MeV using a BW resonance,² resulting in best-fit parameters of $E_r = 2.08(4)$ MeV and $\Gamma_r = 3.9(2)$ MeV. The simulations employed to produce the line shapes for the fitting incorporated the sequential decay process that characterizes this structure (see below). We note that any nonresonant contribution was found to be negligible. The energy and width found here are in line with, but considerably more precise than, those found in earlier $p(^8\text{He}, d)$ experiments [48,57]. By comparing the yields of the $^6\text{He} + n$ and $^4\text{He} + 3n$ channels in the energy range of the present structure, we estimate any potential branching ratio to the $^6\text{He} + n$ channel to be less than 0.1%.

¹ $\frac{d\sigma}{dE_{\alpha 2n}} \propto \frac{\Gamma(E_{\alpha 2n})}{(E_r - E_{\alpha 2n})^2 + [\Gamma(E_{\alpha 2n})/2]^2}$, with $\Gamma(E_{\alpha 2n}) = \Gamma_r \frac{E_{\alpha 2n}^2}{E_r^2}$.
² $\frac{d\sigma}{dE_{\alpha 3n}} \propto \frac{\Gamma(E_{\alpha 3n})}{(E_r - E_{\alpha 3n})^2 + [\Gamma(E_{\alpha 3n})/2]^2}$, with $\Gamma(E_{\alpha 3n}) = \Gamma_r \frac{\sqrt{E_{\alpha 3n}}}{\sqrt{E_r}}$.

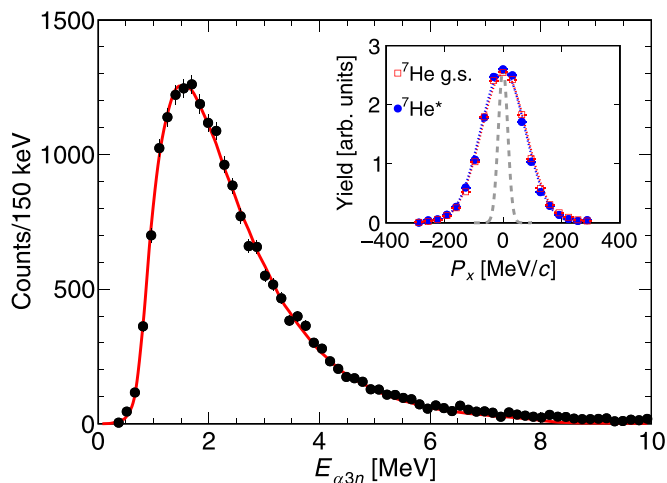


FIG. 3. Relative-energy ($E_{\alpha 3n}$) spectrum for ${}^4\text{He} + 3n$ events. The red solid line shows the best fit up to 5 MeV using a BW line shape (see text). The inset shows the transverse momentum distribution (P_x) of the knocked-out neutron for ${}^7\text{He}$ g.s. [$E_{6\text{He}^* - n} < 1$ MeV in Fig. 2(a)] and for the present ${}^7\text{He}^*$ structure ($1 < E_{\alpha 3n} < 5$ MeV) normalized to the total number of events, with Gaussian fits to the central region to guide the eye. The resolution in P_x (FWHM = 38 MeV/c) is also shown for comparison (dashed line). The vertical error bars are statistical only.

The low-lying states of ${}^7\text{He}$ are expected, based on simple considerations and supported by sophisticated structure model calculations (Table S1 in the Supplemental Material [84]), to arise from a p -shell neutron coupled to the g.s. or 2_1^+ states of ${}^6\text{He}$. Given that the ${}^8\text{He}$ g.s. is dominated by a closed neutron $(p_{3/2})^4$ configuration [57], the most strongly populated level here is, as observed, the ${}^7\text{He}(3/2_1^-)$ g.s. The predicted $1/2^-$ first excited state could, in principle, be populated through neutron removal from the expected small $(p_{3/2})^2(p_{1/2})^2$ configuration, but its strength should be weak, consistent with the lack of any clear signature here for such a state in the ${}^6\text{He} + n$ channel.

As such, the structure observed here at higher energy [$E_x = 2.68(4)$ MeV] in the ${}^4\text{He} + 3n$ channel likely arises from either or both of the predicted $3/2_2^-$ and $5/2_1^-$ levels (Table S1 in the Supplemental Material [84]). The first report of such a structure [48] preferred a $5/2_1^-$ assignment, based on the absence of $3/2_2^-$ built on ${}^6\text{He}^*(2_1^+)$ in RRGm calculations [69]. Subsequent modeling, including those in Table S1 in the Supplemental Material [84], indicates that the exclusion of $3/2_2^-$ was premature. In the current measurement, the momentum distribution for this structure is identical to that for the ${}^7\text{He}$ g.s. (Fig. 3, inset), indicating its production via p -shell neutron knockout. The structure of $5/2_1^-$ (Table S1 in the Supplemental Material [84]) implies that it can only be produced in a two-step process requiring excitation of the ${}^6\text{He}$ core to its 2_1^+ state, while $3/2_2^-$ can be produced directly via the small ${}^6\text{He}(0^+) \otimes p_{3/2}$ admixture. In this context, we note that, excluding the CSM calculations [64], the ratio of the predicted spectroscopic strengths for the ${}^6\text{He}(0^+) \otimes p_{3/2}$ configuration of the $3/2_{1,2}^-$ states is similar to the ratio of their measured efficiency-corrected yields (~ 10). As such, we conclude that the structure observed here arises

predominately from $3/2_2^-$ with a small contribution from $5/2_1^-$ possible.

To further support these arguments, Table S1 in the Supplemental Material [84] includes GSM calculations [88–91] performed for the present study. These calculations incorporate a ${}^4\text{He}$ core and include all partial waves up to $l=3$ for the three valence neutrons. The interactions are adopted from Ref. [68], which employs a Woods-Saxon potential with a spin-orbit term for the core- n one-body interaction and the Furutani-Horiuchi-Tamagaki (FHT) n - n interaction [92,93]. These calculations predict a $5/2_1^-$ level with $E_x = 2.73$ MeV and $3/2_2^-$ with $E_x = 3.37$ MeV, both resonances being rather broad ($\Gamma \sim 2$ – 2.5 MeV) and built predominately on the ${}^6\text{He}(2_1^+) \otimes p_{1/2}$ configuration, with the latter also exhibiting a small ${}^6\text{He}(0^+) \otimes p_{3/2}$ admixture.

The three-neutron system. Turning to the $3n$ system itself, Fig. 4(a) shows for the first time an E_{3n} spectrum reconstructed from the invariant mass of three neutrons for ${}^4\text{He} + 3n$ events with $E_{\alpha 3n} < 5$ MeV. Prior to detailed discussion of possible $3n$ correlations, it is worth examining the relative energy of the ${}^4\text{He} + 2n$ subsystem reconstructed from the ${}^4\text{He} + 3n$ events [Fig. 4(b)], i.e., including all three possible ${}^4\text{He} + 2n$ combinations. The narrow peak at $E_{\alpha 2n} \sim 0.8$ MeV, characteristic of ${}^6\text{He}^*(2_1^+)$, is clearly observed, but superimposed on a much broader component. This suggests that the $3n$ decay is sequential, as in this process one of the three ${}^4\text{He} + 2n$ combinations corresponds to the feeding of ${}^6\text{He}^*(2_1^+)$ while the other two, in which one neutron arises from the decay of ${}^7\text{He}^*$ to ${}^6\text{He}^*(2_1^+)$, result in the broader component.

In the following, we compare the relative-energy spectra to four representative decay scenarios using complete GEANT4 simulations described above, each using as input the experimental $E_{\alpha 3n}$ spectrum shown in Fig. 3. All the simulations are normalized according to the total number of events.

(1) “Four-body PS” (orange dashed line): where the decay of ${}^7\text{He}^*$ into ${}^4\text{He} + 3n$ is governed by four-body phase space (PS) without any ${}^4\text{He} - n$ or $n - n$ final state interactions (FSI).

(2) “Trineutron”: where the decay is initially two-body into ${}^4\text{He} + {}^3n$, using the trineutron resonance parameters predicted by NCGSM [12] ($E_{3n} = 1.3$ MeV and $\Gamma_{3n} = 0.9$ MeV). The 3n then undergoes three-body PS decay without any ${}^4\text{He} - n$ or $n - n$ FSI. For comparison, the “Broad Trineutron” case is also considered (green dashed line), with trineutron resonance parameters obtained from a fit to the experimental E_{3n} spectrum.

(3) “Sequential” (blue dash-dotted line): where the first step is a two-body decay into ${}^6\text{He}^*(2_1^+) + n$, using the ${}^6\text{He}^*(2_1^+)$ resonance parameters obtained above. The subsequent decay of ${}^6\text{He}^*(2_1^+)$ into ${}^4\text{He} + 2n$ is modeled as a pure three-body PS process, without any ${}^4\text{He} - n$ or $n - n$ FSI.

(4) “Sequential- nn ” (red solid line): the “Sequential” scenario with the addition of the effects of the $n - n$ interaction in the decay of ${}^6\text{He}^*(2_1^+)$, included as the emission of the neutron pair in an s -wave virtual state [94] ($a_s = -18.7$ fm [95]). No ${}^4\text{He} - n$ FSI is included. Such a scenario is consistent with the strong $n - n$ correlations exhibited by the ${}^4\text{He} + 2n$ events (Fig. S3 in the Supplemental Material [84]).

The E_{3n} spectrum [Fig. 4(a)], which exhibits a broad structure peaking at around 1 MeV, is well described by all the

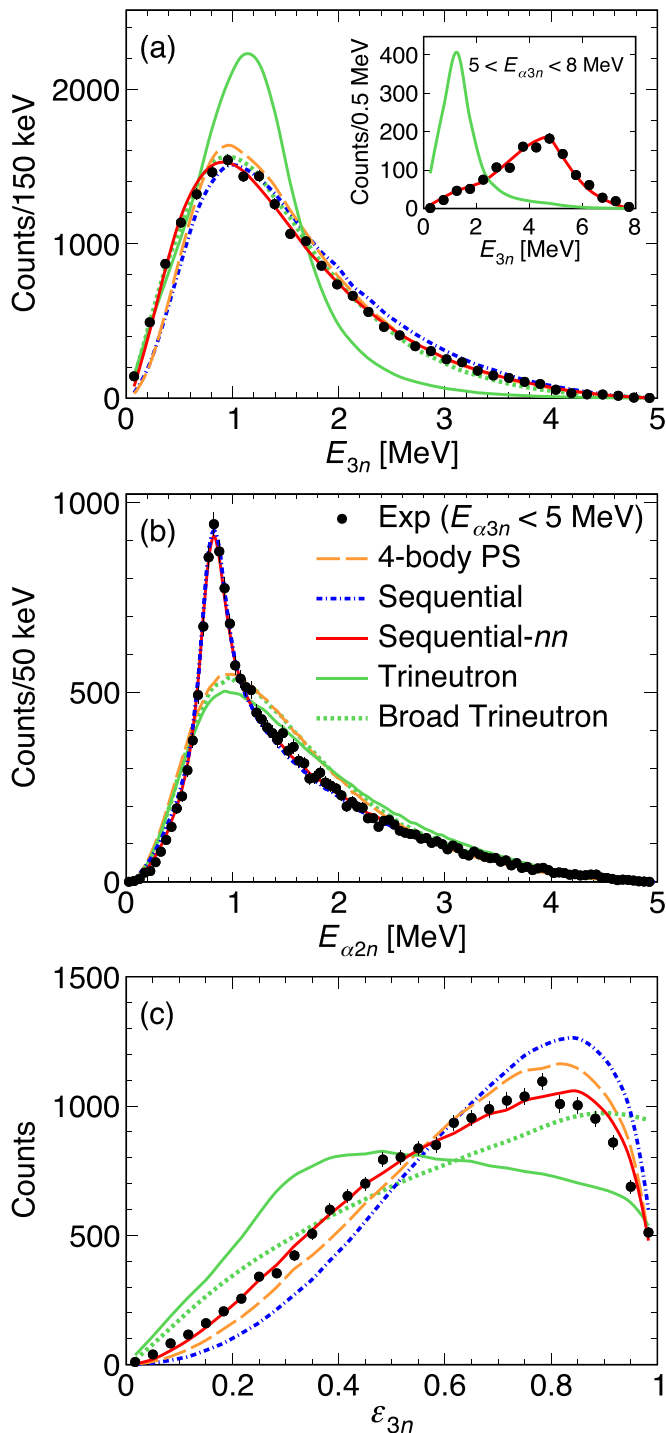


FIG. 4. Relative-energy spectra for ${}^4\text{He}+3n$ events with $E_{\alpha 3n} < 5$ MeV: (a) $3n$ energy E_{3n} ; (b) energy, $E_{\alpha 2n}$, of the ${}^4\text{He}+2n$ subsystem for the ${}^4\text{He}+3n$ events; and (c) normalized $3n$ energy $\epsilon_{3n} = E_{3n}/E_{\alpha 3n}$. The lines correspond to simulations of different decay scenarios (see text). The inset of panel (a) shows the E_{3n} spectrum for events with $5 \text{ MeV} < E_{\alpha 3n} < 8 \text{ MeV}$. The vertical error bars are statistical only.

scenarios except “Trineutron,” which, as expected, is much narrower, reflecting the relatively narrow intrinsic width of the predicted resonance [12]. This difference is further amplified when events from the high-energy tail of ${}^7\text{He}^*$ ($5 \text{ MeV} <$

$E_{\alpha 3n} < 8 \text{ MeV}$) are considered, as shown in the inset of Fig. 4(a). We also note that other trineutron resonance parameters ($E_{3n} = 0.35 \text{ MeV}$ and $\Gamma_{3n} = 0.7 \text{ MeV}$; $E_{3n} = 0.5 \text{ MeV}$ and $\Gamma_{3n} = 1 \text{ MeV}$) predicted by NCSM [15] yield similarly narrow E_{3n} distributions, with peaks even closer to the threshold.

Clearly, the $E_{\alpha 2n}$ spectrum of the ${}^4\text{He}+2n$ subsystem [Fig. 4(b)] is only consistent with the two sequential decay scenarios. Direct emission of the three neutrons, either via four-body phase space or as a trineutron resonance, cannot reproduce the prominent peak at $E_{\alpha 2n} \approx 0.8 \text{ MeV}$, which arises from decay via ${}^6\text{He}^*(2_1^+)$. For “Trineutron,” while better agreement with the E_{3n} spectrum can be achieved by broadening the assumed trineutron resonance in the simulation (“Broad Trineutron” shown as the green dashed line in Fig. 4), it remains impossible to reproduce the very peaked distribution that characterizes the $E_{\alpha 2n}$ spectrum nor can the ϵ_{3n} (see below) spectrum be described. We have also verified that the sequential decay via the ${}^5\text{He}$ g.s. resonance does not play a measurable role and, indeed, no evidence is seen for its formation (Fig. S3 in the Supplemental Material [84]). The $3n$ decay of the ${}^7\text{He}^*$ structure observed here is thus predominantly sequential via ${}^6\text{He}^*(2_1^+)$.

Regarding the two sequential scenarios, the shape of the E_{3n} spectrum [Fig. 4(a)] is better reproduced by including the n - n interaction (“Sequential- nn ”) that shifts the distribution slightly toward lower energies.

In Fig. 4(c), we display the normalized $3n$ energy $\epsilon_{3n} = E_{3n}/E_{\alpha 3n}$, defined as the ratio of the $3n$ energy to the total energy. This variable rescales the $3n$ energy spectrum to a normalized range from 0 to 1 and, as shown, is more sensitive to the different scenarios. Again, the sequential scenario incorporating the n - n interaction (“Sequential- nn ”) in the ${}^6\text{He}^*(2_1^+)$ decay provides the best description.

Finally, we performed a χ^2 fit to the $E_{\alpha 2n}$ spectrum using a combination of “Sequential- nn ” and “Trineutron” in order to set an upper limit for the latter, yielding 0.8% at the 1σ level. If we consider a broader trineutron resonance (“Broad Trineutron”: $E_{3n} = 3 \text{ MeV}$ and $\Gamma_{3n} = 5 \text{ MeV}$) that matches more closely the E_{3n} spectrum of Fig. 4(a), an upper limit of 1.6% can be set. Note that a further increase in the resonance width, such as the broad $3n$ structure reported recently in a measurement of the ${}^3\text{H}(t, {}^3\text{H})3n$ reaction ($\Gamma_{3n} \approx 15 \text{ MeV}$) [16], leads to an even smaller upper limit.

It is therefore concluded that the $3n$ emission from the ${}^7\text{He}^*$ structure observed here is consistent with a purely sequential process via ${}^6\text{He}^*(2_1^+)$. In addition, no evidence is found for a narrow, relatively low-lying trineutron resonance such as that predicted [10,12,15]. While significant two-body neutron correlations are observed in the decay of ${}^6\text{He}^*(2_1^+)$, similar to those observed in the dissociation of ${}^6\text{He}$ [96] and in the ${}^3\text{H}(\pi^-, \gamma)3n$ reaction [17], no evidence is found for any significant $3n$ correlations.

Conclusions. In summary, $3n$ emission from ${}^7\text{He}$ has been directly measured for the first time. A prominent resonance-like structure lying $2.08(4) \text{ MeV}$ above the ${}^4\text{He}+3n$ threshold with a width of $3.9(2) \text{ MeV}$ was observed. Based on the momentum distribution of the knocked-out neutron and comparison with state-of-the-art structure model calculations, it was attributed to arising predominantly from the predicted $3/2_2^-$ excited state of ${}^7\text{He}$ with a possible admixture

from $5/2_1^-$. The $3n$ invariant-mass spectrum and the underlying neutron correlations were investigated. A broad structure peaking at around 1 MeV was observed in the E_{3n} spectrum and, combined with the $E_{\alpha 2n}$ spectrum and complete simulations incorporating n - n correlations, was very well reproduced by the sequential decay of ${}^7\text{He}^*$ via ${}^6\text{He}^*(2_1^+)$. No evidence was found for any significant three-neutron correlations, including any signature of a trineutron resonance. The high-quality three-neutron-emission data reported here could provide a benchmark for theoretical descriptions of multineutron correlations and decay mechanisms of unbound neutron-rich systems.

The present work underlines that direct multineutron detection and the subsequent neutron correlation analyses hold much promise for understanding the structure of multineutron unbound states and the nature of multineutron systems. Such measurements are being extended to other multineutron emitters, such as $4n$ unbound ${}^7\text{H}$.

Acknowledgments. We would like to thank the RIBF accelerator staff for the primary beam delivery and the BigRIPS team for their efforts in preparing the secondary beams. Instructive discussions with Professor Tetsuo Noro (Kyushu University) are gratefully acknowledged. S.W.H. and Z.H.Y. acknowledge the support from the National Key R&D Program of China (Grants No. 2023YFE0101500 and No. 2022YFA1605100) and the National Natural Science Foundation of China (Grant No. 12275006). The LPC Caen participants acknowledges partial support from the French-Japanese LIA-International Associated Laboratory for Nuclear Structure Problems as well as the French

ANR14-CE33-0022-02 EXPAND. P.J.L. acknowledges the support from the National Natural Science Foundation of China (Grant No. 12405147). T.U. acknowledges support from the Grants-in-Aid of the Japan Society for the Promotion of Science (Grant No. JP21H04975). This project was supported by Deutsche Forschungsgemeinschaft (DFG, German Research Foundation), Project-ID 279384907—SFB 1245, the GSI-TU Darmstadt cooperation agreement, the JSPS A3 Foresight Program, JSPS KAKENHI Grants No. JP24H00006 and No. JP18H05404, the Institute for Basic Science (IBS-R031-D1), BMBF (05P24PK1), and the State Key Laboratory of Nuclear Physics and Technology, Peking University (No. NPT2024ZX01, No. NPT2025ZX02). S.P. acknowledges support by the UK STFC under Contracts No. ST/P003885/1 and No. ST/L005727/1 and the University of York Pump Priming Fund. S.W.H. also acknowledges the support from the International Program Associate of RIKEN and the National Research Foundation of Korea (NRF) and the Ministry of Science and ICT (RS-2024-00436392). P.M.P. acknowledges support from the FAIR-RO/RD/2024_011. I.G. has been supported by HIC for FAIR and Croatian Science Foundation (HRZZ) under project no IP-2025-02-2414. R.G. acknowledges support from the BMBF (05P24PK1, 05P24WO2).

Data availability. The data that support the findings of this article are not publicly available upon publication because it is not technically feasible and/or the cost of preparing, depositing, and hosting the data would be prohibitive within the terms of this research project. The data are available from the authors upon reasonable request.

-
- [1] Y. Ye, X. Yang, H. Sakurai, and B. Hu, Physics of exotic nuclei, *Nat. Rev. Phys.* **7**, 21 (2025).
- [2] F. M. Marqués, *et al.*, Detection of neutron clusters, *Phys. Rev. C* **65**, 044006 (2002).
- [3] F. M. Marqués, *et al.*, On the possible detection of $4n$ events in the breakup of ${}^{14}\text{Be}$, [arXiv:nucl-ex/0504009](https://arxiv.org/abs/nucl-ex/0504009).
- [4] F. M. Marqués and J. Carbonell, The quest for light multineutron systems, *Eur. Phys. J. A* **57**, 105 (2021).
- [5] S. W. Huang and Z. H. Yang, Neutron clusters in nuclear systems, *Front. Phys.* **11**, 1233175 (2023).
- [6] K. Kisamori, *et al.*, Candidate resonant tetraneutron state populated by the ${}^4\text{He}({}^8\text{He}, {}^8\text{Be})$ reaction, *Phys. Rev. Lett.* **116**, 052501 (2016).
- [7] M. Duer, *et al.*, Observation of a correlated free four-neutron system, *Nature (London)* **606**, 678 (2022).
- [8] S. C. Pieper, Can modern nuclear Hamiltonians tolerate a bound tetraneutron? *Phys. Rev. Lett.* **90**, 252501 (2003).
- [9] A. M. Shirokov, G. Papadimitriou, A. I. Mazur, I. A. Mazur, R. Roth, and J. P. Vary, Prediction for a four-neutron resonance, *Phys. Rev. Lett.* **117**, 182502 (2016).
- [10] S. Gandolfi, H. W. Hammer, P. Klos, J. E. Lynn, and A. Schwenk, Is a trineutron resonance lower in energy than a tetraneutron resonance? *Phys. Rev. Lett.* **118**, 232501 (2017).
- [11] K. Fosse, J. Rotureau, N. Michel, and M. Ploszajczak, Can tetraneutron be a narrow resonance? *Phys. Rev. Lett.* **119**, 032501 (2017).
- [12] J. G. Li, N. Michel, B. S. Hu, W. Zuo, and F. R. Xu, *Ab initio* no-core Gamow shell-model calculations of multineutron systems, *Phys. Rev. C* **100**, 054313 (2019).
- [13] R. Lazauskas, E. Hiyama, and J. Carbonell, Low energy structures in nuclear reactions with $4n$ in the final state, *Phys. Rev. Lett.* **130**, 102501 (2023).
- [14] I. A. Muzalevskii, *et al.*, Population of tetraneutron continuum in reactions of ${}^8\text{He}$ on deuterium, *Phys. Rev. C* **111**, 014612 (2025).
- [15] I. A. Mazur, M. K. Efimenko, A. I. Mazur, I. J. Shin, V. A. Kulikov, A. M. Shirokov, and J. P. Vary, Trineutron resonances in the SS-HORSE extension of the no-core shell model, *Phys. Rev. C* **110**, 014004 (2024).
- [16] K. Miki, *et al.*, Precise spectroscopy of the $3n$ and $3p$ systems via the ${}^3\text{H}(t, {}^3\text{He})3n$ and ${}^3\text{He}({}^3\text{He}, t)3p$ reactions at intermediate energies, *Phys. Rev. Lett.* **133**, 012501 (2024).
- [17] J. P. Miller, J. A. Bistirlich, K. M. Crowe, S. S. Rosenblum, P. C. Rowe, F. T. Shively, E. R. Grilly, E. C. Kerr, J. Novak, R. H. Sherman, H. Brändle, G. Strassner, and P. Trüöl, Upper limits for bound states and resonance behavior in the trineutron system, *Nucl. Phys. A* **343**, 347 (1980).
- [18] L. Zhou, S. M. Wang, D. Q. Fang, and Y. G. Ma, Recent progress in two-proton radioactivity, *Nucl. Sci. Tech.* **33**, 105 (2022).
- [19] M. Pfützner, I. Mukha, and S. M. Wang, Two-proton emission and related phenomena, *Prog. Part. Nucl. Phys.* **132**, 104050 (2023).

- [20] Z. Kohley, J. Snyder, T. Baumann, G. Christian, P. A. DeYoung, J. E. Finck, R. A. Haring-Kaye, M. Jones, E. Lunderberg, B. Luther, S. Mosby, A. Simon, J. K. Smith, A. Spyrou, S. L. Stephenson, and M. Thoennessen, Unresolved question of the ^{10}He ground state resonance, *Phys. Rev. Lett.* **109**, 232501 (2012).
- [21] A. Spyrou, Z. Kohley, T. Baumann, D. Bazin, B. A. Brown, G. Christian, P. A. DeYoung, J. E. Finck, N. Frank, E. Lunderberg, S. Mosby, W. A. Peters, A. Schiller, J. K. Smith, J. Snyder, M. J. Strongman, M. Thoennessen, and A. Volya, First observation of ground state dineutron decay: ^{16}Be , *Phys. Rev. Lett.* **108**, 102501 (2012).
- [22] Z. Kohley, E. Lunderberg, P. A. DeYoung, A. Volya, T. Baumann, D. Bazin, G. Christian, N. L. Cooper, N. Frank, A. Gade, C. Hall, J. Hinefeld, B. Luther, S. Mosby, W. A. Peters, J. K. Smith, J. Snyder, A. Spyrou, and M. Thoennessen, First observation of the ^{13}Li ground state, *Phys. Rev. C* **87**, 011304 (2013).
- [23] Y. Kondo, *et al.*, Nucleus ^{26}O : A barely unbound system beyond the drip line, *Phys. Rev. Lett.* **116**, 102503 (2016).
- [24] B. Monteagudo, *et al.*, Mass, spectroscopy, and two-neutron decay of ^{16}Be , *Phys. Rev. Lett.* **132**, 082501 (2024).
- [25] R. A. Kryger, A. Azhari, M. Hellström, J. H. Kelley, T. Kubo, R. Pfaff, E. Ramakrishnan, B. M. Sherrill, M. Thoennessen, S. Yokoyama, R. J. Charity, J. Dempsey, A. Kirov, N. Robertson, D. G. Sarantites, L. G. Sobotka, and J. A. Winger, Two-proton emission from the ground state of ^{12}O , *Phys. Rev. Lett.* **74**, 860 (1995).
- [26] I. Mukha, *et al.*, Observation of two-proton radioactivity of ^{19}Mg by tracking the decay products, *Phys. Rev. Lett.* **99**, 182501 (2007).
- [27] I. A. Egorova, *et al.*, Democratic decay of ^6Be exposed by correlations, *Phys. Rev. Lett.* **109**, 202502 (2012).
- [28] F. Wamers, *et al.*, First observation of the unbound nucleus ^{15}Ne , *Phys. Rev. Lett.* **112**, 132502 (2014).
- [29] K. W. Brown, R. J. Charity, L. G. Sobotka, Z. Chajceki, L. V. Grigorenko, I. A. Egorova, Yu. L. Parfenova, M. V. Zhukov, S. Bedoor, W. W. Buhro, J. M. Elson, W. G. Lynch, J. Manfredi, D. G. McNeel, W. Reviol, R. Shane, R. H. Showalter, M. B. Tsang, J. R. Winkelbauer, and A. H. Wuosmaa, Observation of long-range three-body Coulomb effects in the decay of ^{16}Ne , *Phys. Rev. Lett.* **113**, 232501 (2014).
- [30] T. B. Webb, *et al.*, First observation of unbound ^{11}O , the mirror of the halo nucleus ^{11}Li , *Phys. Rev. Lett.* **122**, 122501 (2019).
- [31] R. J. Charity, *et al.*, Investigations of three-, four-, and five-particle decay channels of levels in light nuclei created using a ^9C beam, *Phys. Rev. C* **84**, 014320 (2011).
- [32] R. J. Charity, *et al.*, Observation of the exotic isotope ^{13}F located four neutrons beyond the proton drip line, *Phys. Rev. Lett.* **126**, 132501 (2021).
- [33] K. W. Brown, R. J. Charity, J. M. Elson, W. Reviol, L. G. Sobotka, W. W. Buhro, Z. Chajceki, W. G. Lynch, J. Manfredi, R. Shane, R. H. Showalter, M. B. Tsang, D. Weisshaar, J. R. Winkelbauer, S. Bedoor, and A. H. Wuosmaa, Proton-decaying states in light nuclei and the first observation of ^{17}Na , *Phys. Rev. C* **95**, 044326 (2017).
- [34] D. Kostyleva, *et al.*, Towards the limits of existence of nuclear structure: Observation and first spectroscopy of the isotope ^{31}K by measuring its three-proton decay, *Phys. Rev. Lett.* **123**, 092502 (2019).
- [35] X.-D. Xu, *et al.*, Isospin symmetry breaking disclosed in the decay of three-proton emitter ^{20}Al , *Phys. Rev. Lett.* **135**, 022502 (2025).
- [36] R. J. Charity, J. M. Elson, J. Manfredi, R. Shane, L. G. Sobotka, Z. Chajceki, D. Coupland, H. Iwasaki, M. Kilburn, J. Lee, W. G. Lynch, A. Sanetullaev, M. B. Tsang, J. Winkelbauer, M. Youngs, S. T. Marley, D. V. Shetty, A. H. Wuosmaa, T. K. Ghosh, and M. E. Howard, $2p$ - $2p$ decay of ^8C and isospin-allowed $2p$ decay of the isobaric-analog state in ^8B , *Phys. Rev. C* **82**, 041304 (2010).
- [37] Y. Jin, *et al.*, First observation of the four-proton unbound nucleus ^{18}Mg , *Phys. Rev. Lett.* **127**, 262502 (2021).
- [38] Y. Kondo, *et al.*, First observation of ^{28}O , *Nature (London)* **620**, 965 (2023).
- [39] Evidence has also been found for sequential $3n$ decay of ^{25}O [40] and ^{15}Be [41].
- [40] C. Sword, J. Brett, T. Baumann, B. A. Brown, N. Frank, J. Herman, M. D. Jones, H. Karrick, A. N. Kuchera, M. Thoennessen, J. A. Tostevin, M. Tuttle-Timm, and P. A. DeYoung, Observation of three-neutron sequential emission from $^{25}\text{O}^*$, *Phys. Rev. C* **100**, 034323 (2019).
- [41] A. N. Kuchera, R. Shahid, J. Zhao, A. Edmondson, P. A. DeYoung, N. Frank, J. McDonough, O. Peterson-Veach, W. F. Rogers, T. Redpath, and M. Thoennessen, Evidence for the ^{15}Be ground state from ^{12}Be $3n$ events, *Phys. Rev. C* **110**, 064302 (2024).
- [42] G. Papadimitriou, A. T. Kruppa, N. Michel, W. Nazarewicz, M. Ploszajczak, and J. Rotureau, Charge radii and neutron correlations in helium halo nuclei, *Phys. Rev. C* **84**, 051304 (R) (2011).
- [43] Y. L. Sun, *et al.*, Three-body breakup of ^6He and its halo structure, *Phys. Lett. B* **814**, 136072 (2021).
- [44] ENSDF at <https://www.nndc.bnl.gov/>.
- [45] Y. Aksyutina, *et al.*, Properties of the ^7He ground state from ^8He neutron knockout, *Phys. Lett. B* **679**, 191 (2009).
- [46] Z. X. Cao, *et al.*, Recoil proton tagged knockout reaction for ^8He , *Phys. Lett. B* **707**, 46 (2012).
- [47] F. Renzi, *et al.*, Spectroscopy of ^7He using the $^9\text{Be}(^6\text{He}, ^8\text{Be})$ transfer reaction, *Phys. Rev. C* **94**, 024619 (2016).
- [48] A. A. Korshennikov, M. S. Golovkov, A. Ozawa, E. A. Kuzmin, E. Yu. Nikolskii, K. Yoshida, B. G. Novatskii, A. A. Ogloblin, I. Tanihata, Z. Fulop, K. Kusaka, K. Morimoto, H. Otsu, H. Petruscu, and F. Tokanai, Observation of an excited state in ^7He with unusual structure, *Phys. Rev. Lett.* **82**, 3581 (1999).
- [49] A. A. Korshennikov, M. S. Golovkov, A. Ozawa, E. A. Kuzmin, E. Yu. Nikolskii, K. Yoshida, B. G. Novatskii, A. A. Ogloblin, I. Tanihata, Z. Fulop, K. Kusaka, K. Morimoto, H. Otsu, H. Petruscu, and F. Tokanai, Excited state of ^7He and its unique structure, *Phys. Scr.* **2000**, 199 (2000).
- [50] A. H. Wuosmaa, K. E. Rehm, J. P. Greene, D. J. Henderson, R. V. F. Janssens, C. L. Jiang, L. Jisonna, E. F. Moore, R. C. Pardo, M. Paul, D. Peterson, S. C. Pieper, G. Savard, J. P. Schiffer, R. E. Segel, S. Sinha, X. Tang, and R. B. Wiringa, Search for excited states in ^7He with the (d, p) reaction, *Phys. Rev. C* **72**, 061301 (2005).
- [51] A. H. Wuosmaa, *et al.*, Structure of ^7He by proton removal from ^8Li with the $(d, ^3\text{He})$ reaction, *Phys. Rev. C* **78**, 041302(R) (2008).
- [52] G. V. Rogachev, P. Boutachkov, A. Aprahamian, F. D. Bechetti, J. P. Bychowski, Y. Chen, G. Chubarian,

- P. A. DeYoung, V. Z. Goldberg, J. J. Kolata, L. O. Lamm, G. F. Peaslee, M. Quinn, B. B. Skorodumov, and A. Wöhr, Analog states of ${}^7\text{He}$ observed via the ${}^6\text{He}(p, n)$ reaction, *Phys. Rev. Lett.* **92**, 232502 (2004).
- [53] P. Boutachkov, G. V. Rogachev, V. Z. Goldberg, A. Aprahamian, F. D. Becchetti, J. P. Bychowski, Y. Chen, G. Chubarian, P. A. DeYoung, J. J. Kolata, L. O. Lamm, G. F. Peaslee, M. Quinn, B. B. Skorodumov, and A. Wöhr, Doppler shift as a tool for studies of isobaric analog states of neutron-rich nuclei: Application to ${}^7\text{He}$, *Phys. Rev. Lett.* **95**, 132502 (2005).
- [54] F. Beck, D. Frekers, P. von Neumann-Cosel, A. Richter, N. Ryezayeva, and I. J. Thompson, Spectroscopic factor of the ${}^7\text{He}$ ground state, *Phys. Lett. B* **645**, 128 (2007).
- [55] H. G. Bohlen, R. Kalpakchieva, A. Blažević, B. Gebauer, T. N. Massey, W. von Oertzen, S. Thummerer, Spectroscopy of ${}^7\text{He}$ states using the $({}^{15}\text{N}, {}^{17}\text{F})$ reaction on ${}^9\text{Be}$, *Phys. Rev. C* **64**, 024312 (2001).
- [56] M. Meister, *et al.*, Evidence for a new low-lying resonance state in ${}^7\text{He}$, *Phys. Rev. Lett.* **88**, 102501 (2002).
- [57] F. Skaza, *et al.*, Experimental evidence for subshell closure in ${}^8\text{He}$ and indication of a resonant state in ${}^7\text{He}$ below 1 MeV, *Phys. Rev. C* **73**, 044301 (2006).
- [58] S. C. Pieper, R. B. Wiringa, and J. Carlson, Quantum Monte Carlo calculations of excited states in $A = 6-8$ nuclei, *Phys. Rev. C* **70**, 054325 (2004).
- [59] I. A. Mazur, I. J. Shin, Y. Kim, A. I. Mazur, A. M. Shirokov, P. Maris, and J. P. Vary, SS-HORSE extension of the no-core shell model: Application to resonances in ${}^7\text{He}$, *Phys. Rev. C* **106**, 064320 (2022).
- [60] D. M. Rodkin and Y. M. Tchuvil'sky, Detailed theoretical study of the decay properties of states in the ${}^7\text{He}$ nucleus within an *ab initio* approach, *Phys. Rev. C* **104**, 044323 (2021).
- [61] S. Baroni, P. Navrátil, and S. Quaglioni, *Ab initio* description of the exotic unbound ${}^7\text{He}$ nucleus, *Phys. Rev. Lett.* **110**, 022505 (2013).
- [62] S. Baroni, P. Navrátil, and S. Quaglioni, Unified *ab initio* approach to bound and unbound states: No-core shell model with continuum and its application to ${}^7\text{He}$, *Phys. Rev. C* **87**, 034326 (2013).
- [63] A. Volya and V. Zelevinsky, Discrete and continuum spectra in the unified shell model approach, *Phys. Rev. Lett.* **94**, 052501 (2005).
- [64] T. Myo, K. Katō, and K. Ikeda, Resonances of ${}^7\text{He}$ using the complex scaling method, *Phys. Rev. C* **76**, 054309 (2007).
- [65] T. Myo, R. Ando, and K. Katō, One-neutron removal strength of ${}^7\text{He}$ into ${}^6\text{He}$ using the complex scaling method, *Phys. Rev. C* **80**, 014315 (2009).
- [66] J. Rotureau, N. Michel, W. Nazarewicz, M. Płoszajczak, and J. Dukelsky, Density matrix renormalization group approach for many-body open quantum systems, *Phys. Rev. Lett.* **97**, 110603 (2006).
- [67] K. Fosse, J. Rotureau, and W. Nazarewicz, Energy spectrum of neutron-rich helium isotopes: Complex made simple, *Phys. Rev. C* **98**, 061302 (2018).
- [68] Y. Jaganathen, R. M. Id Betan, N. Michel, W. Nazarewicz, and M. Płoszajczak, Quantified Gamow shell model interaction for *psd*-shell nuclei, *Phys. Rev. C* **96**, 054316 (2017).
- [69] J. Wurzer and H. M. Hofmann, Structure of the helium isotopes ${}^4\text{He}$ - ${}^8\text{He}$, *Phys. Rev. C* **55**, 688 (1997).
- [70] R. Lazauskas and J. Carbonell, Three-neutron resonance trajectories for realistic interaction models, *Phys. Rev. C* **71**, 044004 (2005).
- [71] E. Hiyama, R. Lazauskas, J. Carbonell, and M. Kamimura, Possibility of generating a 4-neutron resonance with a $T = 3/2$ isospin 3-neutron force, *Phys. Rev. C* **93**, 044004 (2016).
- [72] S. Ishikawa, Three-neutron bound and continuum states, *Phys. Rev. C* **102**, 034002 (2020).
- [73] M. D. Higgins, C. H. Greene, A. Kievsky, and M. Viviani, Nonresonant density of states enhancement at low energies for three or four neutrons, *Phys. Rev. Lett.* **125**, 052501 (2020).
- [74] T. Kubo, In-flight RI beam separator BigRIPS at RIKEN and elsewhere in Japan, *Nucl. Instrum. Methods Phys. Res. Sect. B* **204**, 97 (2003).
- [75] T. Ohnishi, *et al.*, Identification of 45 new neutron-rich isotopes produced by in-flight fission of a ${}^{238}\text{U}$ beam at 345 MeV/nucleon, *J. Phys. Soc. Jpn.* **79**, 073201 (2010).
- [76] A. Obertelli, *et al.*, MINOS: A vertex tracker coupled to a thick liquid-hydrogen target for in-beam spectroscopy of exotic nuclei, *Eur. Phys. J. A* **50**, 8 (2014).
- [77] C. Santamaria, *et al.*, Tracking with the MINOS time projection chamber, *Nucl. Instrum. Methods Phys. Res. Sect. A* **905**, 138 (2018).
- [78] T. Kobayashi, N. Chiga, T. Isobe, Y. Kondo, T. Kubo, K. Kusaka, T. Motobayashi, T. Nakamura, J. Ohnishi, H. Okuno, H. Otsu, T. Sako, H. Sato, Y. Shimizu, K. Sekiguchi, K. Takahashi, R. Tanaka, and K. Yoneda, SAMURAI spectrometer for RI beam experiments, *Nucl. Instrum. Methods Phys. Res. Sect. B* **317**, 294 (2013).
- [79] H. Sato, T. Kubo, Y. Yano, K. Kusaka, J. Ohnishi, K. Yoneda, Y. Shimizu, T. Motobayashi, H. Otsu, T. Isobe, T. Kobayashi, K. Sekiguchi, T. Nakamura, Y. Kondo, Y. Togano, T. Murakami, T. Tsuchihashi, T. Orikasa, and K. Maeta, Superconducting dipole magnet for SAMURAI spectrometer, *IEEE Trans. Appl. Supercond.* **23**, 4500308 (2013).
- [80] K. Boretzky, *et al.*, NeuLAND: The high-resolution neutron time-of-flight spectrometer for R^3B at FAIR, *Nucl. Instrum. Methods Phys. Res. Sect. A* **1014**, 165701 (2021).
- [81] T. Nakamura and Y. Kondo, Large acceptance spectrometers for invariant mass spectroscopy of exotic nuclei and future developments, *Nucl. Instrum. Methods Phys. Res. Sect. B* **376**, 156 (2016).
- [82] Y. Kondo, T. Tomai, and T. Nakamura, Recent progress and developments for experimental studies with the SAMURAI spectrometer, *Nucl. Instrum. Methods Phys. Res. Sect. B* **463**, 173 (2020).
- [83] S. W. Huang, *et al.*, Experimental study of 4n by directly detecting the decay neutrons, *Few-Body Syst.* **62**, 102 (2021).
- [84] See Supplemental Material at <http://link.aps.org/supplemental/10.1103/sr8h-2n6v> for neutron detection efficiencies, search for excited states in the ${}^6\text{He} + n$ channel, Dalitz plot for the ${}^4\text{He} + 2n$ channel, and table of theoretical predictions for the ${}^7\text{He}$ level structure, which includes Refs. [50,61,62,65,82,85,86].
- [85] G. Cowan, K. Cranmer, E. Gross, and O. Vitells, Asymptotic for likelihood-based tests of new physics, *Eur. Phys. J. C* **71**, 1554 (2011).
- [86] A. Revel, *et al.*, Strong neutron pairing in core $4n$ nuclei, *Phys. Rev. Lett.* **120**, 152504 (2018).

- [87] B. Monteagudo, Structure and neutron decay of the unbound Beryllium isotopes $^{15,16}\text{Be}$, Ph.D. thesis, LPC-Caen, Normandie Université, 2019, <https://theses.hal.science/tel-02518505>.
- [88] N. Michel, W. Nazarewicz, M. Płoszajczak, and K. Bennaceur, Gamow shell model description of neutron-rich nuclei, *Phys. Rev. Lett.* **89**, 042502 (2002).
- [89] N. Michel, W. Nazarewicz, M. Płoszajczak, and T. Vertse, Shell model in the complex energy plane, *J. Phys. G: Nucl. Part. Phys.* **36**, 013101 (2009).
- [90] M. Xie, J. Li, N. Michel, H. Li, S. Wang, H. Ong, and W. Zuo, Investigation of spectroscopic factors of deeply-bound nucleons in drip-line nuclei with the Gamow shell model, *Phys. Lett. B* **839**, 137800 (2023).
- [91] M. Xie, J. Li, N. Michel, H. Li, and W. Zuo, Spectroscopic factors of resonance states with the Gamow shell model, *Sci. China Phys. Mech. Astron.* **67**, 212011 (2024).
- [92] H. Furutani, H. Horiuchi, and R. Tamagaki, Structure of the second 0^+ state of ^4He , *Prog. Theor. Phys.* **60**, 307 (1978).
- [93] H. Furutani, H. Horiuchi, and R. Tamagaki, Cluster-model study of the $T = 1$ states in $A = 4$ system: $^3\text{He} + p$ scattering, *Prog. Theor. Phys.* **62**, 981 (1979).
- [94] H. Esbensen, G. F. Bertsch, and K. Hencken, Application of contact interactions to Borromean halos, *Phys. Rev. C* **56**, 3054 (1997).
- [95] D. E. González Trotter, F. Salinas Meneses, W. Tornow, C. R. Howell, Q. Chen, A. S. Crowell, C. D. Roper, R. L. Walter, D. Schmidt, H. Witała, W. Glöckle, H. Tang, Z. Zhou, and I. Šlaus, Neutron-deuteron breakup experiment at $E_n = 13$ MeV: Determination of the 1S_0 neutron-neutron scattering length a_{nn} , *Phys. Rev. C* **73**, 034001 (2006).
- [96] T. Aumann, *et al.*, Continuum excitations in ^6He , *Phys. Rev. C* **59**, 1252 (1999).